Air Damping in an Ultra-High-Frequency Disk Resonator

L.-Y. Yap*, L.-K. Yap* and W. Ye*

*Woodruff School of Mechanical Engineering,
Georgia Institute of Technology, GA, USA.
wenjing.ye@me.gatech.edu

ABSTRACT

In this paper we investigate the air damping in a circular disk radially oscillating at 1GHz. First the compressibility effects of air between the disk and the substrate are studied. The pressure perturbation along the radial distance is calculated by analytically solving the compressible Navier-Stokes equation. It has been found that the pressure perturbation is 7-order smaller than the ambient pressure. Therefore compressibility effects are negligible. Next, we simulate the energy dissipation due to the air damping by numerically solving the Stokes equation in air that surrounds the disk, electrodes and substrate. The quality factor is then calculated based on the simulation results. For the studied disk, the quality factor is on the order of 10^7 which indicates viscous damping is not a significant loss mechanism.

Keywords: Air damping, Resonator, Boundary Element Method, Navier-Stokes.

1 INTRODUCTION

Micromachined resonators are promising devices for RF applications [1]. To achieve high frequency, instead of shrinking the size of the resonator, an alternative approach is to increase the stiffness of the device. Based on this approach, various designs such as laterally vibrating disk resonator have been proposed and fabricated [1]. One critical issue in resonators is energy dissipation. In order to achieve high quality factor (Q), most devices that have been reported are packaged in vacuum to reduce the energy loss due to air damping. It is, therefore, of interest to investigate whether there is a need for vacuum package. In this paper, we study the air damping on an ultra-high-frequency disk-shape resonator laterally oscillating in air. Figure 1 shows the geometry and dimensions of the studied disk-shape resonator. It consists a vibrating disk, four stationary electrodes with 60° span for each and a stationary substrate. At any point inside the disk, the velocity is prescribed as

$$\vec{V} = r\cos(\omega t)\times 10^6 \vec{e}_r, \qquad (1)$$

where $\vec{e}_r$ is a unit vector in the radial direction , r is the radial distance of that point and ω is the angular frequency that equals $2\pi\times 10^9$ rad/sec.

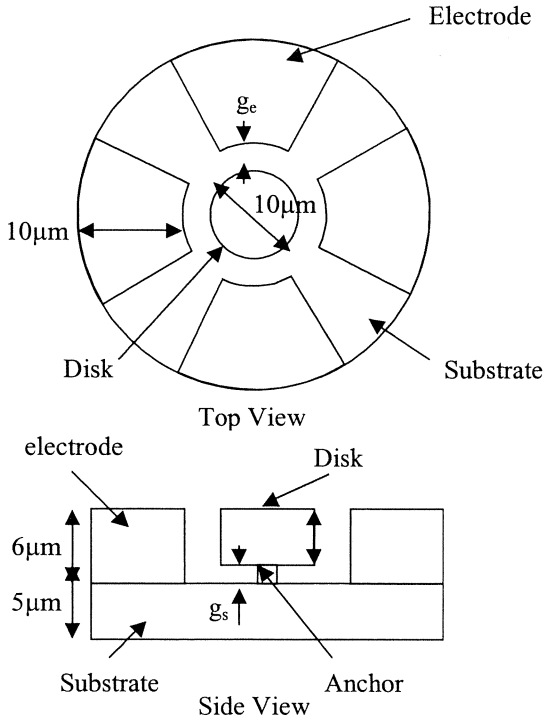

Figure 1. Schematics of a micro resonator.

2 QUALITY FACTOR

The quality factor (Q) of a vibrating system is defined as the ratio of the total stored energy to the energy dissipated in one cycle as shown in Equation (2) [2].

$$Q = \frac{2\pi W}{D} \qquad (2)$$

In Equation (2), W is the total energy stored in the system and D is the energy dissipated in one cycle. In this study, we focus on air damping analysis. Therefore the Q is calculated based on the assumption that air damping is the sole source of the energy dissipation. In this case, D can be calculated from Equation (3).

$$D = \int_s \frac{1}{\omega}\int_0^{2\pi} \vec{f}(\omega t)\cdot\vec{V}(\omega t)d(\omega t)dA \qquad (3)$$

In (3), $\vec{f}$ is the damping force per area acting on the disk due to air and s indicates the surface of the disk. W can be obtained by calculating the total kinetic energy stored in the disk at $t = 0$.

3 DAMPING ANALYSIS

In this study, the smallest characteristic length of air flow surrounding the disk is 1 μm. Therefore the well-known Navier-Stokes equation [3] is employed to analyze the fluid field. For a general flow, the momentum equation reads

$$\frac{\partial(\rho\overline{V})}{\partial t} + \nabla \bullet (\rho\overline{V}\overline{V}) = -\nabla p + \nabla \bullet \tau + \rho B \ , \qquad (4)$$

where $\rho, \overline{V}, p, \tau$ and B refers to the density, velocity , pressure, stress tensor and body force respectively. The continuity equation and the Newtonian-flow assumption are then used to simplify Equation (4) into (5).

$$\rho\frac{\partial\overline{V}}{\partial t} + \rho(\overline{V} \bullet \nabla)\overline{V} = \rho B - \nabla p + \frac{1}{3}\mu\nabla(\nabla \bullet \overline{V}) + \mu\nabla^2\overline{V} \ . \qquad (5)$$

In (5), μ is the fluid viscosity.

To further simplify the governing equation, we first study the air compressibility effects in our resonator. We focus on air between the disk and the substrate since this is where most compressibility effects (if there is any) take place.

3.1 Compressibility Effects

Consider two circular disks with radius of R and gap of h as shown in Figure 2.

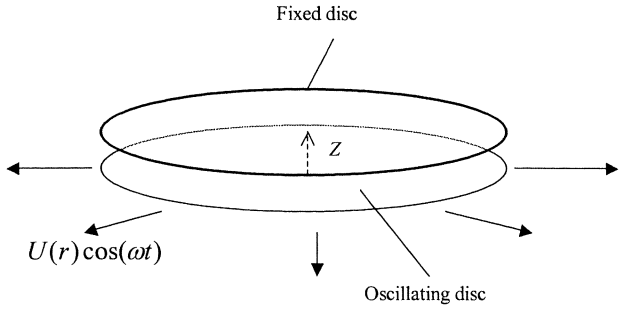

Figure 2. Schematic of two circular disks.

The aspect ratio of $\left(\frac{R}{h}\right)$ is on the order of 5 or up. A dimensional analysis shows $\frac{1}{3}\mu\nabla(\nabla \bullet \overline{V}) + \mu\nabla^2\overline{V}$ can be reduced to $\mu\frac{\partial^2\vec{V}}{\partial z^2}$ because of the high aspect ratio. The nonlinear convective term on the left side of Equation (5) can also be dropped due to the small Reynolds' number associated with the flow. Furthermore, the variation of pressure along z direction is small compared with the variation of pressure along x or y direction. Therefore, the z-direction momentum equation can be neglected. Consequently, Equation (5) is reduced to

x-component $$\rho\frac{\partial u}{\partial t} = -\frac{\partial p}{\partial x} + \mu\frac{\partial^2 u}{\partial z^2} \qquad (6)$$

y-component $$\rho\frac{\partial v}{\partial t} = -\frac{\partial p}{\partial y} + \mu\frac{\partial^2 v}{\partial z^2} \qquad (7)$$

where u and v are the x- and y-components of velocity. The ratio between the inertial term (e.g. $\rho\frac{\partial u}{\partial t}$) in Equations (6) or (7) to the viscous term (e.g. $\mu\frac{\partial^2 u}{\partial z^2}$) is on the order of $\mathrm{Re}\cdot\left(\frac{h}{R}\right)^2$. Therefore, it can also be neglected compared with the viscous term. Finally, the governing equations for air between the disk and substrate are

$$0 = -\frac{\partial p}{\partial x} + \mu\frac{\partial^2 u}{\partial z^2} \qquad (8)$$

$$0 = -\frac{\partial p}{\partial y} + \mu\frac{\partial^2 v}{\partial z^2} \qquad (9)$$

By properly integrating (8), (9) and combining them with equation of state for ideal gas, we can obtain a single equation that depends on the pressure and density as shown in (10).

$$\frac{\partial(\rho u)}{\partial x} + \frac{\partial(\rho v)}{\partial y} = \frac{h^2}{6\mu}\left[\frac{\partial}{\partial x}\left(\rho\frac{\partial P}{\partial x}\right) + \frac{\partial}{\partial y}\left(\rho\frac{\partial P}{\partial y}\right)\right] \qquad (10)$$

In (10), u and v are the amplitudes of x and y components of the velocity of the disk (no-slip boundary condition is assumed).

With the geometry and the boundary conditions (i.e., $u = U(r)\cos\theta, v = U(r)\sin\theta$) as shown in Figure 2, Equation (10) can be reduced to

$$\frac{\partial(\rho U)}{\partial r} = \frac{h^2}{6\mu}\left[\frac{\partial}{\partial r}\left(\rho\frac{\partial P}{\partial r}\right)\right] . \qquad (11)$$

For the case of $U(r) = r$, Equation (11) is further reduced to

$$\frac{\partial P}{\partial r}r + P = \frac{h^2}{6\mu}\left[\left(\frac{\partial P}{\partial r}\right)^2 + P\frac{\partial^2 P}{\partial r^2}\right] . \qquad (12)$$

Assume $P = P_a + \delta P$, $\delta \mathrm{P} << \mathrm{P}$, where P_a is the ambient pressure. Equation (12) can then be linearized to a non-dimensional form shown in (13).

$$\frac{h^2 P_a}{6\mu R^2}\left(\frac{\partial^2\delta p'}{\delta r'^2}\right) - r\left(\frac{\partial\delta p'}{\delta r'}\right) - \delta p' = 1 \qquad (13)$$

This equation can then be solved analytically with the boundary conditions of $\delta P' = 0$ at $r' = 1$, and $\frac{\partial \delta P'}{\partial r'} = 0$ at $r' = 0$.

Figure 3 shows the radial distribution of the normalized pressure pertubation. Compared with the ambient pressure, the perturbation is on the order of 10^{-7}. This fact indicates the air compressiblity effects is insignificant and therefore, an incompressible flow model is adequate to analyze the damping caused by air.

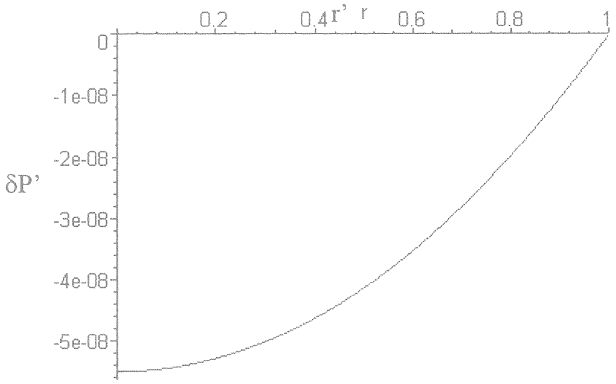

Figure 3. Radial distribution of pressure pertubation.

3.2 Viscous Damping Analysis

Since the compressibility effects are negligible, the incompressible Navier-Stokes equation is employed to analyze the fluid field (air). Due to small Reynolds number, the Navier-Stokes equation can be further reduced to the Stokes equation shown in (14).

$$\rho \frac{\partial \overline{V}}{\partial t} = -\nabla p + \mu \nabla^2 \overline{V} \qquad (14)$$

To solve Equation (14) together with the continuity equation in air surrounding the resonator, we apply a 3-D fast Stokes solver developed in house [4,5] to find the traction force acting on the disk due to air. This solver uses the Boundary Element Method (BEM) [6] to solve the boundary integral equations that are equivalent to the Stokes equation. A collocation scheme is employed. The surface of the structure (the disk, electrodes and substrate) is discretized into *n* panels. On each panel, the components of the velocity and the traction force are assumed to be constant. A system of equations for the unknowns is then derived by insisting that the integral equation is satisfied exactly at each panel centroid. The result is a linear system which relates the known quantities (velocity $\vec{u}$) to the unknown quantities (traction force $\vec{f}$). This dense system is then solved using the GMRES iterative solver [7]. To accelerate the linear solver, a pre-corrected FFT technique is employed [8] for quickly computing approximate matrix-vector products. The result is a fast and yet accurate algorithm. The fast Stokes solver has been successfully applied to analyze the air damping in a laterally oscillating micro resonator (translation-mode)[9].

Figure 4 shows a discretized disk together with stationary electrodes and substrate.

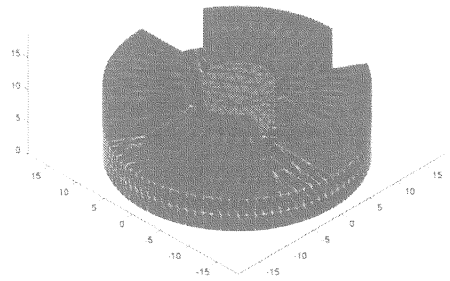

Figure 4. A discretized disk, electrodes and substrate.

3.2.1 Translating Mode

A disk moving at a constant velocity is considered first. Drag forces per velocity acting on the disk at different gap between the disk and electrodes are recorded in Table 1. The total drag force is broken down into three components, namely top force (force due to air on top of the oscillating disk), bottom force (force came from air between the disk and the substrate) and side force (force acting on the side of the oscillating disk).

Table 1. Drag force per velocity for a translating disk (10^{-10})

g_e (μm)	Top	Bottom	Side	Drag
1	0.091	0.43	3.59	4.1
2	0.075	0.27	1.25	1.59
5	0.060	0.19	0.41	0.65
10	0.048	0.24	0.24	0.53

For the smallest g_e shown in Table 1, the corresponding Q value is on the order of 3×10^6. The relationships of the drag force versus the diameter and the height of the disk are also studied and results are shown in Figures 5 and 6. In both cases, the drag force increases almost linearly with the increasing diameter and height.

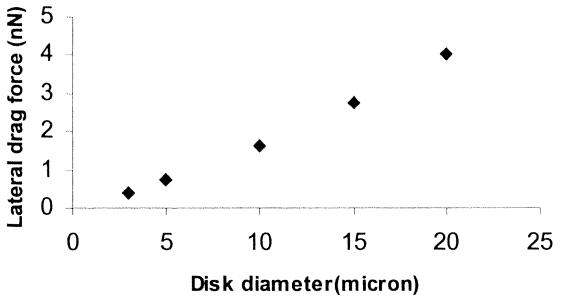

Figure 5. Drag force versus diameter of the disk.

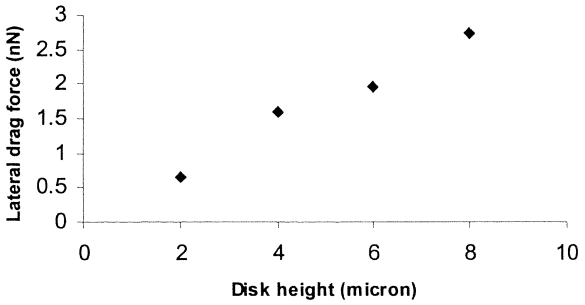

Figure 6. Drag force versus height of the disk.

It is also interesting to note that the design of different electrodes has impact on the drag force. Table 2 shows the drag forces on the device with different number of electrodes while the total overlap area between the electrodes and disk is fixed.

Table 2. Drag on a disk with a fixed overlap area between disk and electrodes (10^{-10}).

No. of electrodes	Drag
8	1.82
4	1.59
2	1.39

3.2.2 Radially Oscillating Mode

Here, we consider a disk oscillating at a velocity described in (1). The simulated traction forces are substituted into Equation (3) to compute the energy dissipated via air (D). Results are shown in Table 1, together with the stored energy W and the quality factor (Q).

Table 1. Quality factors of a radially oscillating disk with different gaps between the disk and the electrodes.

g_e (μm)	D (10^{-18} J)	W (10^{-13} J)	Q (10^6)
1	0.0283	2.55	25.52
2	0.0286	2.55	25.25
5	0.0277	2.55	26.07
10	0.00735	2.55	98.25

4 CONCLUSION

In this paper we investigate the air damping in a circular disk radially oscillating at 1GHz. First the compressibility effects of air between the disk and the substrate are studied. The pressure perturbation along the radial distance is calculated by analytically solving the compressible Navier-Stokes equation. It has been found that the pressure perturbation is 7-order smaller than the ambient pressure. Therefore compressibility effects are negligible. Next, we simulate the energy dissipation due to the air damping by numerically solving the Stokes equation in air that surrounds the disk, electrodes and substrate. The quality factor is then calculated based on the simulation results. For the studied disk, the quality factor is on the order of 10^7 which indicates viscous damping is not a significant loss mechanism.

REFERENCES

[1] Clark, J. R., Hsu, W.-T. and Clark, T.-C. Nguyen, "High-Q VHF Micromechanical Contour-Mode Disk Resonator," *Technical Digest*, IEEE Int. Electron Devices Meeting, San Francisco, California, Dec. 11-13, 2000, pp. 493-496.

[2] Cho, Y-H, Pisano, A. and Howe, R. T., "Viscous Damping Model for Laterally Oscillating Microstructures," *Journal of Microelectromechanical Systems*, Vol. 3, No. 2, 1994, pp. 81 – 87.

[3] Panton, R. L., (1996), *Incompressible Flow*, Second edition, Wiley-Interscience, NY.

[4] W. Ye, X. Wang and J. White, "A Fast 3D Solver for Unsteady Flow with Applications to Micro-Electro-Mechanical Systems," *Proc. of the International Conference on Modeling and Simulation of Microsystems, Semiconductors, Sensors and Actuators,* pp. 518 – 521, 1999.

[5] W. Ye, X. Wang and J. White, "A Fast Stokes Solver for Generalized Flow Problems," *Proc. of the International Conference on Modeling and Simulation of Microsystems, Semiconductors, Sensors and Actuators,* pp. 524 – 527, 2000.

[6] P. K. Banerjee, *The Boundary Element Methods in Engineering*, McGraw-Hill Book Company, England, 1981.

[7] Y. Saad and M. Schultz, "GMRES: A generalized minimal residual algorithm for solving symmetric linear systems", *SIAM, J. Sci. Statis. Comput.*, Vol. 7, pp. 856 - 869, 1986.

[8] Phillips, J. R. and White, J., 1997, "A Precorrected-FFT Method for Electrostatic Analysis of Complicated 3-D Structures," *IEEE Trans. On CAD*, Vol. 16, No. 10, pp.1059 – 1072.

[9] W. Ye, X. Wang, W. Hemmert, D. Freeman and J. White, "Viscous Drag on a Lateral Micro-resonator: Fast 3-D Fluid Simulation and Measurement Data", *Hilton Head Workshop: Sensors and Actuators,* pp. 124 – 127, 2000.